

HIGH-POWER DC-DC CONVERTER FOR ELECTRICAL VEHICLE APPLICATIONS

P. Mamatha¹, G. Pranay Kumar²

¹ Student, Dept of EEE, Vaageswari college of Engineering, Telangana, India

² Asst.Prof, Dept of EEE, Vaageswari college of Engineering, Telangana, India

ABSTRACT

This paper presents a hybrid-type full-bridge dc/dc converter for renewable energy applications. Two different control schemes with a simple circuit structure, the proposed dc/dc converter has hybrid operation modes. Under a normal input range, the proposed converter operates as a phase-shift full-bridge series-resonant converter that provides high efficiency by applying soft switching on all switches and rectifier diodes and reducing conduction losses. When the input is lower than the normal input range, the converter operates as an active-clamp step-up converter that enhances an operation range. Due to the hybrid operation, the proposed converter operates with larger phase-shift value than the conventional converters under the normal input range. Thus, the proposed converter is capable of being designed to give high power conversion efficiency and its operation range is extended. A Solar PV system is fed at the input of dc/dc converter and analyzed for both low power applications and high power applications. The Proposed system is designed in MATLAB software for analysis.

Keyword: - Active-clamp circuit, full-bridge circuit, phase shift control, ZVS, ZCS.

1. INTRODUCTION

The demands for dc/dc converters with a high power density, high efficiency, and low electromagnetic interference (EMI) have been increased in various industrial fields in recent days. As the switching frequency increases to obtain high power density, switching losses related to the turn-on and turn-off of the switching devices increase. Because these losses limit the increase of the switching frequency, soft switching techniques are indispensable. Among previous dc/dc converters, a phase-shift full-bridge (PSFB) converter is attractive because all primary switches are turned on with zero-voltage switching (ZVS) without additional auxiliary circuits [1]. However, the PSFB converter has some serious problems such as narrow ZVS range of lagging-leg switches, high power losses by circulating current, and voltage ringing across rectifier diodes. Especially, with a requirement of wide input range, the PSFB converter is designed to operate with small phase-shift value under the normal input range; the design of the PSFB converter lengthens the freewheeling interval and causes the excessive circulating current which increases conduction losses [2], [3].

Active-clamp circuits have been commonly used to absorb surge energy stored in leakage inductance of a transformer. Moreover, the circuits provide a soft switching technique [4], [5]. Some studies have introduced dc/dc converters combining the active-clamp circuit and voltage doubler or multiplier rectifier [6], [7]. The circuit configuration allows achieving a step-up function like a boost converter. The voltage stresses of rectifier diodes are also clamped at the output voltage and no extra snubber circuit is required.

In this paper, a novel hybrid-type full-bridge (FB) dc/dc converter with high efficiency is proposed; the converter is derived from a combination of a PSFB series-resonant converter and an active-clamp step-up converter with a voltage doubler circuit. Using a hybrid control scheme with a simple circuit structure, the proposed converter has two operation modes.[8] Under the normal input range, the proposed converter operates as a PSFB series-resonant converter. The proposed converter yields high efficiency by applying soft switching techniques on all the primary switches and rectifier diodes and by reducing conduction losses. When the input voltage is lower than the normal input range, the converter operates as an active-clamp step-up converter.[9] In this mode, the proposed converter provides a step-up function by using the active-clamp circuit on the primary side and the voltage doubler rectifier on the secondary side. Finally, simulation analysis of the proposed converter is done using MATLAB software.



Fig-1: Block diagram of proposed system

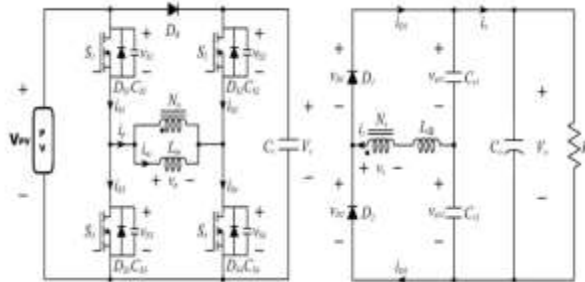


Fig-2: Circuit diagram of the proposed hybrid-type full-bridge dc/dc converter.

2. PRINCIPLE OPERATION OF THE PROPOSED CONVERTER

The Fig. 2 shows a circuit diagram of the proposed converter. On the primary side of the power transformer T , the proposed converter has an FB circuit with one blocking diode DB and one clamp capacitor Cc . On the secondary side, there is a voltage doubler rectifier. The operation of the proposed converter can be classified into two cases. One is a PSFB series-resonant converter mode.

The proposed converter operates in two modes:

- 1) PSFB Series-Resonant Converter Mode
- 2) Active-Clamp Step-Up Converter Mode

2.1 PSFB Series-Resonant Converter Mode

Under the normal input voltage range, the proposed converter is operated by phase-shift control. In this mode, Vc is the same as the input voltage Vd and DB is conducted. All switches are driven with a constant duty ratio 0.5 and short dead time. Figs. 2 and 3 show the operation waveforms and equivalent circuits, respectively. A detailed mode analysis is given as four modes.

Mode 1 [t_0, t_1]: Prior to t_0 , the switches S_1 and S_2 are in on state and the secondary current i_s is zero. The primary current i_p flows through DB , S_1 , S_2 , and Lm . During this mode, the primary voltage v_p and secondary voltage v_s of the transformer T are zero. Thus, the magnetizing current i_m is constant and satisfies as follows:

$$i_m(t) = i_p(t) = i_m(t_0). \tag{1}$$

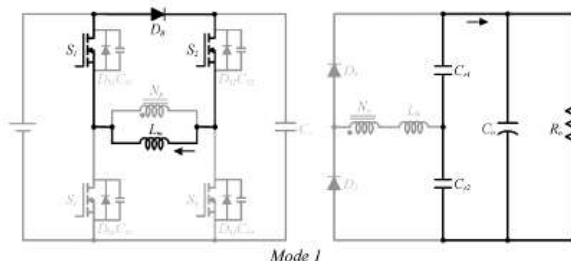


Fig-3: PSFB resonant converter at mode 1

Mode 2 [t_1, t_2]: At t_1 , S_2 is turned off. Because i_p flowing through S_2 is very low, S_2 is turned off with near zero-current. In this mode, i_p charges CS_2 and discharges CS_4 .

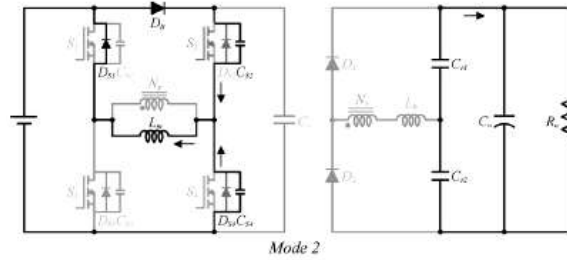


Fig-4: PSFB resonant converter at mode2

Mode 3 [t2, t3]: At t2, the voltage across S4 reaches zero. At the same time, ip flows through the body diode DS4. Thus, S4 is turned on with zero-voltage while DS4 is conducted. In this mode, vs is nVd where the turn ratio n of the transformer is given by Ns/Np and the secondary current is begins to flow through D1. The state equation of this mode is written as follows:

$$L_{lk} \frac{di_p(t)}{dt} = nV_d - V_{cr1}(t) \quad (2)$$

$$i_s = C_{r1} \frac{dV_{cr1}(t)}{dt} - C_{r2} \frac{dV_{cr2}(t)}{dt} \quad (3)$$

where vcr1 and vcr2 are the voltages across Cr1 and Cr2, respectively. Since Vo is constant, the secondary current is can be obtained as

$$i_s(t) = C_{r2} \frac{dV_{cr1}(t)}{dt} - C_{r2} \frac{d(V_o - V_{cr1}(t))}{dt} = C_r \frac{dV_{cr1}(t)}{dt} \quad (4)$$

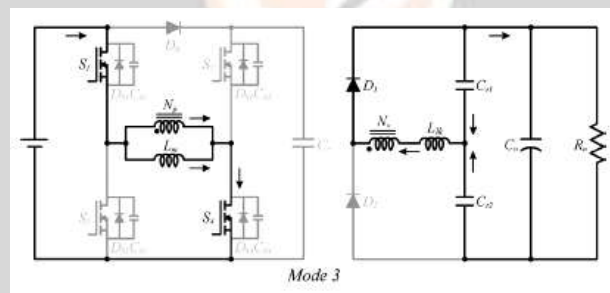


Fig-5: PSFB resonant converter at mode 3

Where the equivalent resonant capacitance Cr is Cr1+ Cr2. Using (2) and (4), the secondary current is can be calculated as

$$i_s(t) = \frac{nV_d - V_{cr1}(t)}{Z_r} \sin \omega_r(t - t_2) \quad (5)$$

The angular frequency ωr and characteristic impedance Zr are given by

$$\omega_r = \frac{1}{\sqrt{L_{lk} C_r}}, \quad Z_r = \sqrt{\frac{L_{lk}}{C_r}} \quad (6)$$

Meanwhile, the magnetizing current im increases linearly as follows:

$$i_m(t) = i_m(t) + \frac{V_d}{L_m}(t - t_2) \quad (7)$$

In this mode, power is transferred from the input to the output.

Mode 4 [t3, t4]: This mode begins when S1 is turned off. The primary current ip charges CS1 and discharges CS3. When the voltage across S3 becomes zero, ip flows through the body diode DS3. Thus, S3 is turned on with zero-voltage while DS3 is conducted. When vp is zero, D1 is still conducted and -vcr1 is applied to Llk. Thus, the secondary current is goes to zero rapidly. In the end of this mode, since the secondary current is close to zero before D1 is reverse bias, the losses by the reverse recovery problem are small as negligible. Since operations during the next half switching period are similar with Mode 1-4, explanations of Mode 5-8 are not presented.

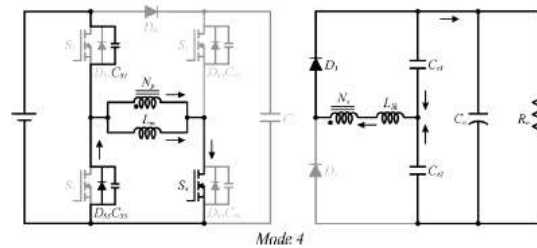


Fig-6: PSFB resonant converter at mode4

2.2 Active-Clamp Step-Up Converter Mode

As the input voltage decreases up to a certain minimum value of the normal input range, the phase-shift value ϕ increases up to its maximum value, 1. If the input voltage is lower than the minimum value of the normal input range, the proposed converter is operated by dual asymmetrical pulse width modulation (PWM) control. The switches (S1 , S4) and (S2 , S3) are treated as switch pairs and operated complementarily with short dead time. The duty D over 0.5 is based on (S1 , S4) pair. In this situation, the clamp capacitor voltage V_c is higher than V_d . Then, the blocking diode DB is reverse biased and the proposed converter operates as the active-clamp step-up converter. Figs. 4 and 5 show the operation waveforms and equivalent circuits in the active-clamp step-up converter mode, respectively.

Mode 1 [t0 , t1]: At t0 , S1 and S4 are turned on. Since V_d is applied to L_m , the magnetizing current i_m is linearly increased and is expressed as

$$i_m(t) = i_m(t_0) + \frac{V_d}{L_m}(t - t_0) \tag{8}$$

D1 is conducted and the secondary current i_s begins to resonate by L_{lk} , $Cr1$, and $Cr2$. In this mode, the state equation is written as follows:

$$L_{lk} \frac{di_s(t)}{dt} = nV_d - V_{Cr1}(t) \tag{9}$$

$$i_s(t) = C_{r1} \frac{dV_{Cr1}(t)}{dt} - C_{r2} \frac{dV_{Cr2}(t)}{dt} = C_r \frac{dV_{Cr1}(t)}{dt} \tag{10}$$

From (9) and (10), the secondary current i_s can be calculated as

$$i_s(t) = i_s(t_2) \csc \omega_r(t - t_2) - \frac{nV_d - V_{Cr2}(t_2)}{Z_r} \sin \omega_r(t - t_2) \tag{11}$$

In this mode, power is transferred from the input to the output.

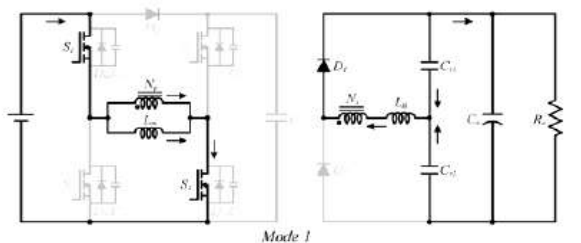


Fig-8: active clamp step up converter at mode1

Mode 2 [t1 , t2]: At t1, S1 and S4 are turned off. The primary current i_p charges and discharges the output capacitors of the switches during very short time.

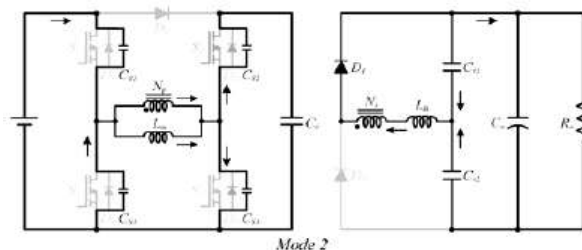


Fig-9: active clamp step up converter at mode2

Mode 3 [t2, t3]: This mode begins when the voltages across S2 and S3 are zero. At the same time, ip flows through DS2 and DS3. Thus, S2 and S3 are turned on with zero-voltage. Since the negative voltage -Vc is applied to Lm, the magnetizing current im decreases linearly as

$$i_m(t) = i_m(t_2) - \frac{V_c}{L_m}(t - t_2) \quad (12)$$

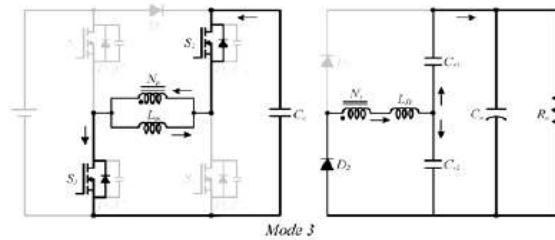


Fig-10: active clamp step up converter at mode3

In this mode, the secondary current is begins to second resonance and the state equation is written as follows:

$$L_{lk} \frac{di_s}{dt} = V_{cr2}(t) - nV_c \quad (13)$$

$$i_s(t) = C_{r1} \frac{dV_{cr1}(t)}{dt} - C_{cr2} \frac{dV_{cr2}(t)}{dt} = -C_r \frac{dV_{cr2}(t)}{dt} \quad (14)$$

Using (13) and (14), the secondary current is given by

$$i_s(t) = i_s(t_2) \cos \omega_r(t - t_2) - \frac{nV_c - V_{cr2}(t_2)}{Z_r} \sin \omega_r(t - t_2) \quad (15).$$

Mode 4 [t3, t4]: At t3, S2 and S3 are turned off. The primary current ip charges CS2, CS3 and discharges CS1, CS4 during very short time.

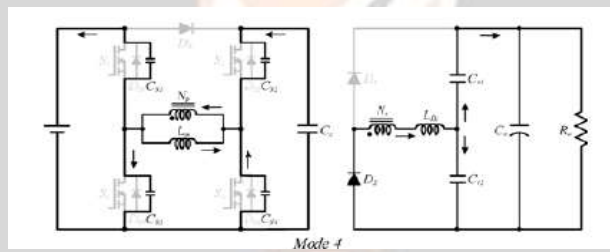


Fig-11: active clamp step up converter at mode4

3. RESULTS AND ANALYSIS

The proposed system is designed using MATLAB/SIMULINK software for theoretical analysis. To show the proposed system as efficient the proposed system is operated in two modes as resonant mode and active mode.

3.1 Proposed System with Solar PV system in Phase shifted mode

The Fig-12 to fig-17 represents the resonant mode of the proposed system using solar photovoltaic mode. During phase shifted or resonant mode the output requirement is low so it operate with high dwell time.

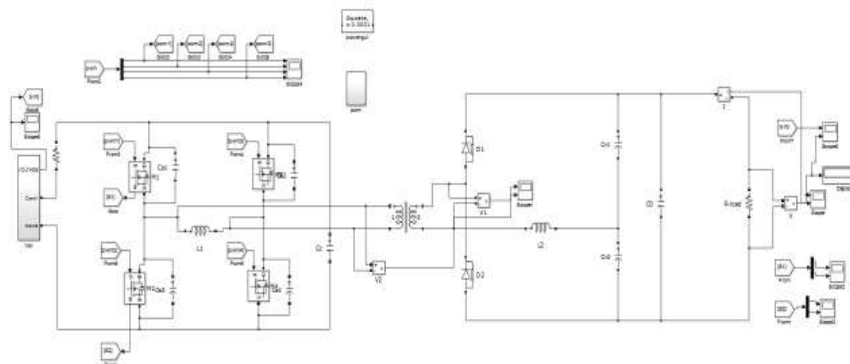


Fig-12: Matlab design of proposed system without Solar system

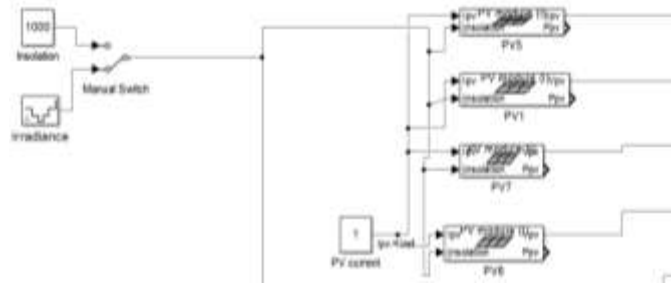


Fig-13: Solar PV model in MATLAB

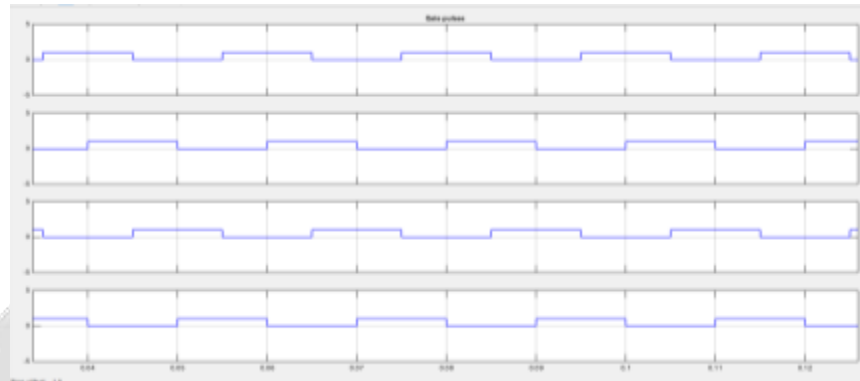


Fig-14: PWM Pulses for Phase shifted mode

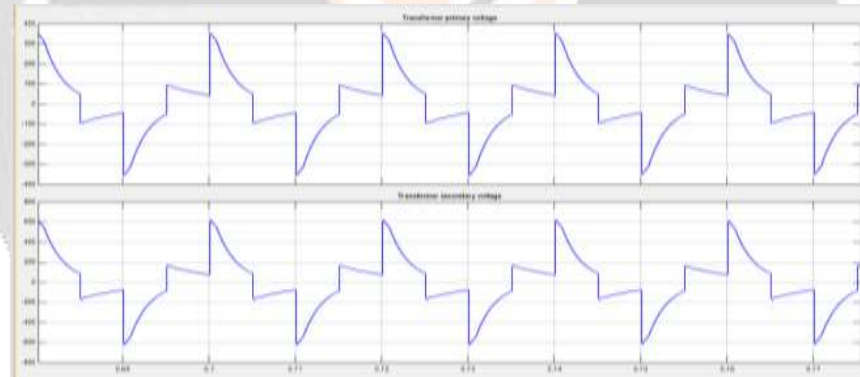


Fig-15: Transformer primary and secondary voltages

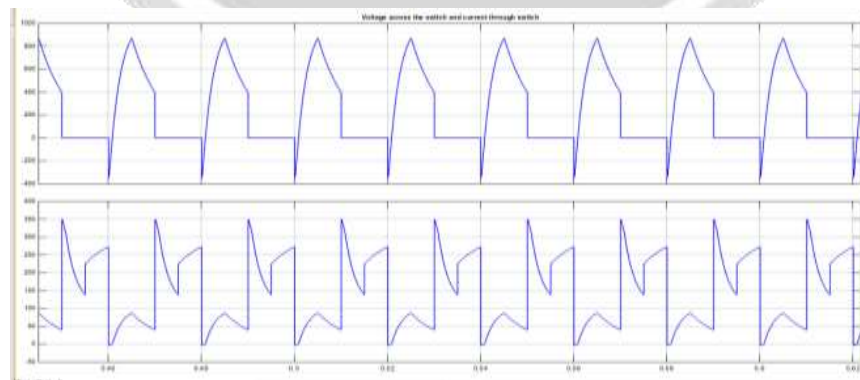


Fig-16: voltage and current of switch s 1

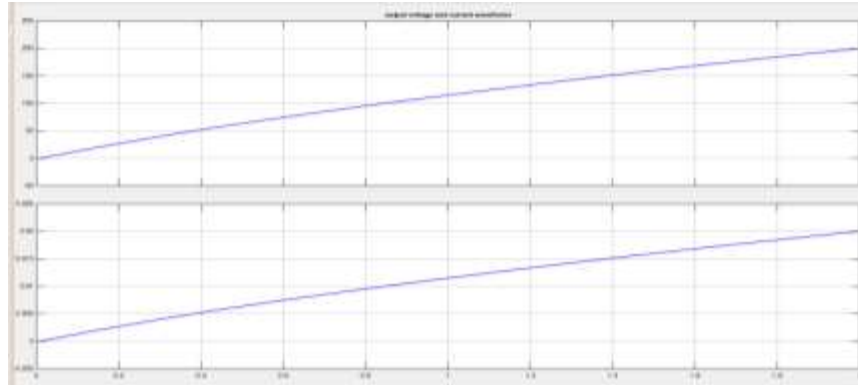


Fig-17: output voltage and current of the proposed system

3.2 Proposed System with Solar PV system in Active clamp mode

The fig.18 to 23 shows the outputs of solar PV system in active clamp mode. For different insolation the output is constant and maximum.

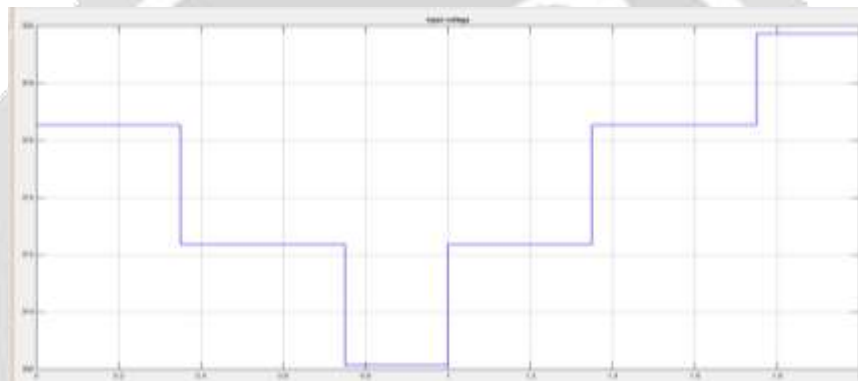


Fig-18: Solar PV output fed to proposed converter



Fig-19: PWM pulses to proposed converter

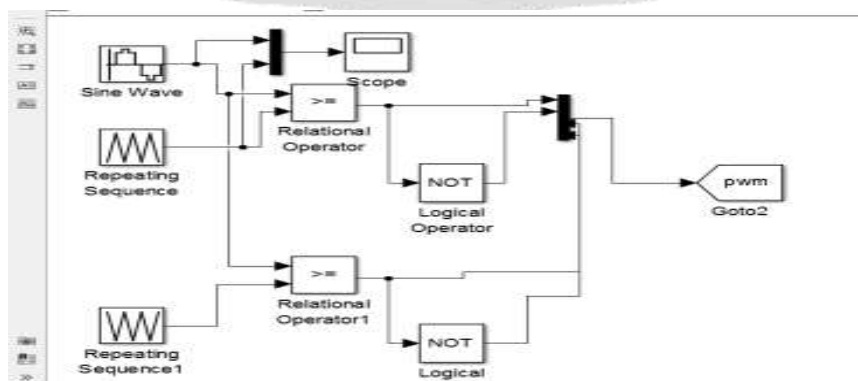


Fig-20: PWM technique

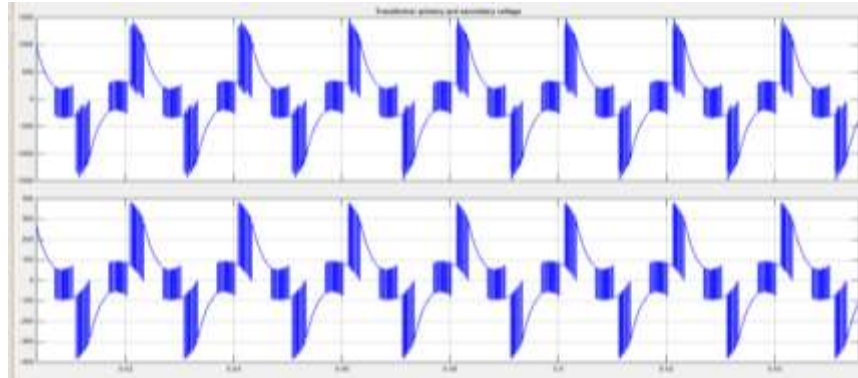


Fig-21: Transformer primary and secondary voltages

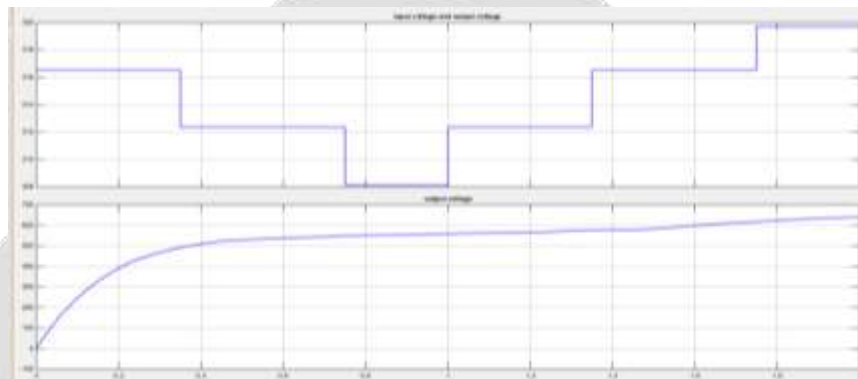


Fig-22: input voltage versus output voltage

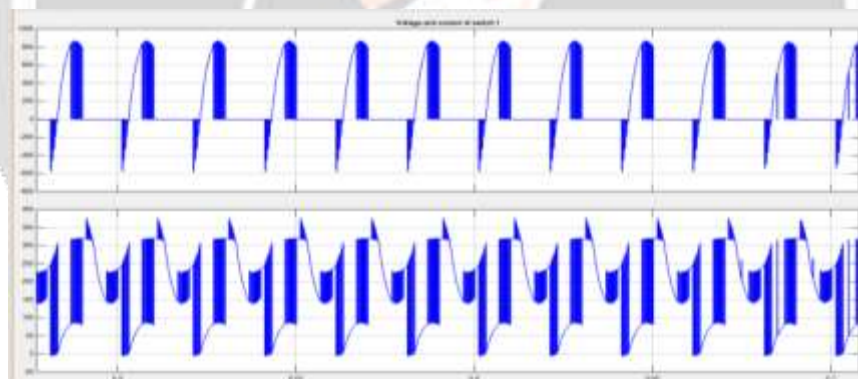


Fig-23: voltage and current of switch 1

4. CONCLUSIONS

The novel hybrid-type full-bridge dc/dc converter with high efficiency has been simulated for analysis. By using the hybrid control scheme with the simple circuit structure, the proposed converter has both the step-down and step-up functions, which ensure to cover the wide input range. Under the normal input range, the proposed converter achieves high efficiency by providing soft switching technique to all the switches and rectifier diodes, and reducing the current stress. When the input is lower than the normal input range, the proposed converter provides the step-up function by using the active-clamp circuit and voltage doubler, which extends the operation range. To confirm the validity of the proposed converter, MATLAB simulations have carried out. Under the normal input range, the conversion efficiency is over 96% at full-load condition, and the input range from 250 to 350 V is guaranteed. Thus, the proposed converter has many advantages such as high efficiency and wide input range.

6. REFERENCES

- [1] J. A. Sabat'e, V. Vlatkovic, R. B. Ridley, F. C. Lee, and B. H. Cho, "Design considerations for high-voltage high-power full-bridge zero-voltage switching PWM converter," in *Proc. Appl. Power Electron. Conf.*, 1990, pp. 275–284.
- [2] I. O. Lee and G. W. Moon, "Phase-shifted PWM converter with a wide ZVS range and reduced circulating current," *IEEE Trans. Power Electron.*, vol. 28, no. 2, pp. 908–919, Feb. 2013.
- [3] Y. S. Shin, S. S. Hong, D. J. Kim, D. S. Oh, and S. K. Han, "A new changeable full bridge dc/dc converter for wide input voltage range," in *Proc. 8th Int. Conf. Power Electron. ECCE Asia*, May 2011, pp. 2328–2335.
- [4] P. K. Jain, W., Kang, H. Soin, and Y. Xi, "Analysis and design considerations of a load and line independent zero voltage switching full bridge dc/dc converter topology," *IEEE Trans. Power Electron.*, vol. 17, no. 5, pp. 649–657, Sep. 2002.
- [5] I. O. Lee and G. W. Moon, "Soft-switching DC/DC converter with a full ZVS range and reduced output filter for high-voltage application," *IEEE Trans. Power Electron.*, vol. 28, no. 1, pp. 112–122, Jan. 2013.
- [6] G. N. B. Yadav and N. L. Narasamma, "An active soft switched phase shifted full-bridge dc-dc converter: Analysis, modeling, design, and implementation," *IEEE Trans. Power Electron.*, vol. 29, no. 9, pp. 4538–4550, Sep. 2014.
- [7] Y. Jang, M. M. Jovanović, and Y.-M. Chang, "A new ZVS-PWM full-bridge converter," *IEEE Trans. Power Electron.*, vol. 18, no. 5, pp. 1122–1129, Sep. 2003.
- [8] T. T. Song and N. Huang, "A novel zero-voltage and zero-current switching full-bridge PWM converter," *IEEE Trans. Power Electron.*, vol. 20, no. 2, pp. 286–291, Mar. 2005.
- [9] R. Huang and S. K. Mazumder, "A soft-switching scheme for an isolated dc/dc converter with pulsating dc output for a three-phase high-frequency link PWM converter," *IEEE Trans. Power Electron.*, vol. 24, no. 10, pp. 2276–2288, Oct. 2009.